

# Oligomer Characterization of 4–23 kDa Polymers by Electropray Fourier Transform Mass Spectrometry

Peter B. O'Connor and Fred W. McLafferty\*

Contribution from the Department of Chemistry, Baker Laboratory, Cornell University, Ithaca, New York 14853

Received June 28, 1995<sup>®</sup>

**Abstract:** Poly(ethylene glycol)s of 4.3, 13, and 23 kDa give mass spectra containing resolved isotopic peaks representing the individual oligomers in each sample. Approximately 5000 isotopic peaks of 47 oligomers in 10 charge states are identified in the 23 kDa spectrum, as well as <0.02%  $-\text{CH}_2\text{CH}(\text{CH}_3)\text{O}-$  monomer units in the 13 kDa spectrum. As an unexpected advantage of electropray ionization (ESI), the degree of mass discrimination is much less than that of mass/charge discrimination due to averaging of the values from different charge states. For the determination of molecular weight distributions, geometric and entropy deconvolution methods yield unacceptable artifact peaks and abundance discrimination, respectively; combining their deconvolution attributes with isotopic peak restrictions for the 4.3 kDa polymer yields a distribution similar to that from human data reduction, which is consistent with that from GPC separation. ESI/FTMS spectra of polymers can be measured in minutes and provide far more detailed mass information than that from such conventional techniques.

## Introduction

Most polymeric materials are complex mixtures of oligomers, so that their properties such as tensile strength, refractive index, and intrinsic viscosity result from the combined effects of the properties of the individual components. Most methods of relative molecular weight ( $M_r$ ) characterization of these individual components are based on some indirect property, such as the scattering of light or the binding affinity to a stationary phase, that requires calibration with known, preferably monodisperse, standards.<sup>1</sup> In contrast, mass spectrometry (MS) makes possible direct determination of individual oligomers based on their measured  $M_r$  values, with any additional mass values providing evidence of copolymers and impurities.<sup>2–8</sup> MS methodology extending these capabilities with unit resolution

to far larger polymers is described here, with reduced mass discrimination providing more accurate  $M_r$  values, which in turn give far more accurate weight- and number-average distributions ( $M_w$ ,  $M_n$ ) and polydispersity values.

Polymer ionization for MS presents challenging problems. Different oligomer molecules must be ionized and analyzed with similar efficiencies and minimal dissociation. Ionization methods reported include Field Desorption (FD),<sup>2</sup> Fast Atom Bombardment,<sup>3</sup> Desorption Chemical Ionization,<sup>4</sup> Secondary Ion Mass Spectrometry,<sup>5</sup> <sup>252</sup>Cf Plasma Desorption,<sup>6</sup> Laser Desorption,<sup>7</sup> and Matrix Assisted Laser Desorption/Ionization (MALDI).<sup>8</sup> Resolved oligomeric peaks have been obtained by FD for polystyrene as large as 11 kDa<sup>2a</sup> and by MALDI for poly(ethylene glycol) (PEG) as large as 10 kDa,<sup>8c</sup> requiring a resolving power (RP) of 100 (11000/104) and 200 (10000/44), respectively. Most methods (not FD) add excess energy to the ionized molecule, producing dissociation products<sup>8f,g</sup> that require higher RP for mass separation, especially with multiply-charged ESI spectra<sup>9,10</sup> (however, MS of dissociation products from high  $M_r$  materials can supply monomer and/or oligomer fragment information).<sup>5,6</sup> MS instrumentation also has challenging problems, such as mass range limitations, marginal resolution ( $10^2$ – $10^3$  RP of quadrupole and time-of-flight mass spectrometers),<sup>8,10</sup> and mass discrimination<sup>8,10</sup> ( $>2\times$  effect of mass on measurement response).<sup>8f–h,10e</sup>

Electrospray ionization (ESI)<sup>9</sup> has several inherent advantages, including minimal fragmentation and high ionization efficiency,<sup>9,10</sup> and the multiplicity of charges ( $z$ ) placed on each ion by ESI yields a high mass ( $m$ ) range even for limited  $m/z$  range analyzers.<sup>10b,c</sup> Even 5 MDa PEG samples have yielded unresolved<sup>10b</sup> and single ion<sup>10c</sup> ESI mass spectra. However,

<sup>®</sup> Abstract published in *Advance ACS Abstracts*, December 1, 1995.

(1) Hindenlang, D. M.; Sedgwick, R. D. In *Comprehensive Polymer Science*, 1st ed.; Allen, G., Bevington, J. C., Eds.; Pergamon Press: Oxford, 1989; Vol. 1, pp 573–588.

(2) (a) Matsuo, T.; Matsuda, H.; Katakuse, I. *Anal. Chem.* **1979**, *51*, 1329–1331. (b) Jardine, D. R.; Nekula, S.; Than-Trong, N.; Haddad, P. R.; Derrick, P. J. *Macromolecules* **1986**, *19*, 1772–1779. Prókai, L. *Field Desorption Mass Spectrometry*; Marcel Dekker: New York, 1990; Vol. 9.

(3) Lattimer, R. P. *Int. J. Mass Spectrom. Ion Processes* **1984**, *55*, 221; **1992**, *116*, 23–26.

(4) Vincenti, M.; Pelizzetti, E.; Guarini, A.; Costanzi, S. *Anal. Chem.* **1992**, *64*, 1879–1884.

(5) Bletsos, I. V.; Hercules, D. M.; Van Leyden, D.; Hagenhoff, B.; Niehuis, E.; Benninghoven, A. *Anal. Chem.* **1991**, *63*, 1953–1960.

(6) Macfarlane, R. D. *Trends Anal. Chem.* **1988**, *7*, 179–183. Loo, J. A.; Wang, B. H.; Wang, F. C.-Y.; McLafferty, F. W. *Macromolecules* **1987**, *20*, 698–702. Cox, B. D.; Park, M. A.; Kaercher, R. G.; Schweikert, E. A. *Anal. Chem.* **1992**, *64*, 843–847.

(7) Wilkins, C. L.; Weil, D. A.; Yang, C. L. C.; Ijames, C. F. *Anal. Chem.* **1985**, *57*, 520–524. Brenna, J. T.; Creasy, W. R. *Appl. Spectrosc.* **1991**, *45*, 80–91. Kahr, M. S.; Wilkins, C. L. *J. Am. Soc. Mass Spectrom.* **1993**, *4*, 453–460.

(8) (a) Nuwaysir, L. M.; Wilkins, C. L. In *Lasers in Mass Spectrometry*, Oxford Series in Optical Science; Clarendon Press: Oxford, 1990; Vol. 1, pp 291. (b) Bahr, U.; Deppe, A.; Karas, M.; Hillenkamp, F.; Giessmann, U. *Anal. Chem.* **1992**, *64*, 2866–2869. (c) Bürger, H. M.; Müller, H.; Seebach, D.; Börsen, K. O.; Schär, M.; Widmer, H. M. *Macromolecules* **1993**, *26*, 4783–4790. (d) Danis, P. O.; Karr, D. E.; Simonsick, W. J., Jr.; Wu, D. T. *Macromolecules* **1995**, *28*, 1229–1232. (e) Dey, M.; Castoro, J. A.; Wilkins, C. L. *Anal. Chem.* **1995**, *67*, 1575–1579. (f) Lehrle, R. S.; Sarson, D. S. *Rapid Commun. Mass Spectrom.* **1995**, *9*, 91–92. (g) Tang, X.; Dreifus, P. A.; Vertes, A. *Rapid Commun. Mass Spectrom.* **1995**, *9*, 1141–1147. (h) Farmer, T. B.; Caprioli, R. M. *J. Mass Spectrom.* **1995**, *30*, 1245–1254.

(9) Whitehouse, C. M.; Dreyer, R. N.; Yamashita, M.; Fenn, J. B. *Anal. Chem.* **1985**, *57*, 675–679. Smith, R. D.; Loo, J. A.; Ogorzalek-Loo, R. A.; Busman, M.; Udseth, H. R. *Mass Spectrom. Rev.* **1991**, *10*, 359–451. Feng, R.; Konishi, Y. *Anal. Chem.* **1993**, *65*, 645–649.

(10) (a) Smith, R. D.; Loo, J. A.; Edmonds, C. G.; Barinaga, C. J.; Udseth, H. R. *Anal. Chem.* **1990**, *62*, 882–889. (b) Nohmi, T.; Fenn, J. B. *J. Am. Chem. Soc.* **1992**, *114*, 3241–3246. (c) Smith, R. D.; Cheng, X.; Bruce, J. E.; Hofstadler, S. A.; Anderson, G. A. *Nature* **1994**, *369*, 137–139. (d) Sherrard, K. B.; Marriott, P. J.; McCormick, M. J.; Colton, R.; Smith, G. *Anal. Chem.* **1994**, *66*, 3394–3399. (e) Hendrickson, C. L.; Drader, J. J.; Laude, D. A. *J. Am. Soc. Mass Spectrom.* **1995**, *6*, 76–79.

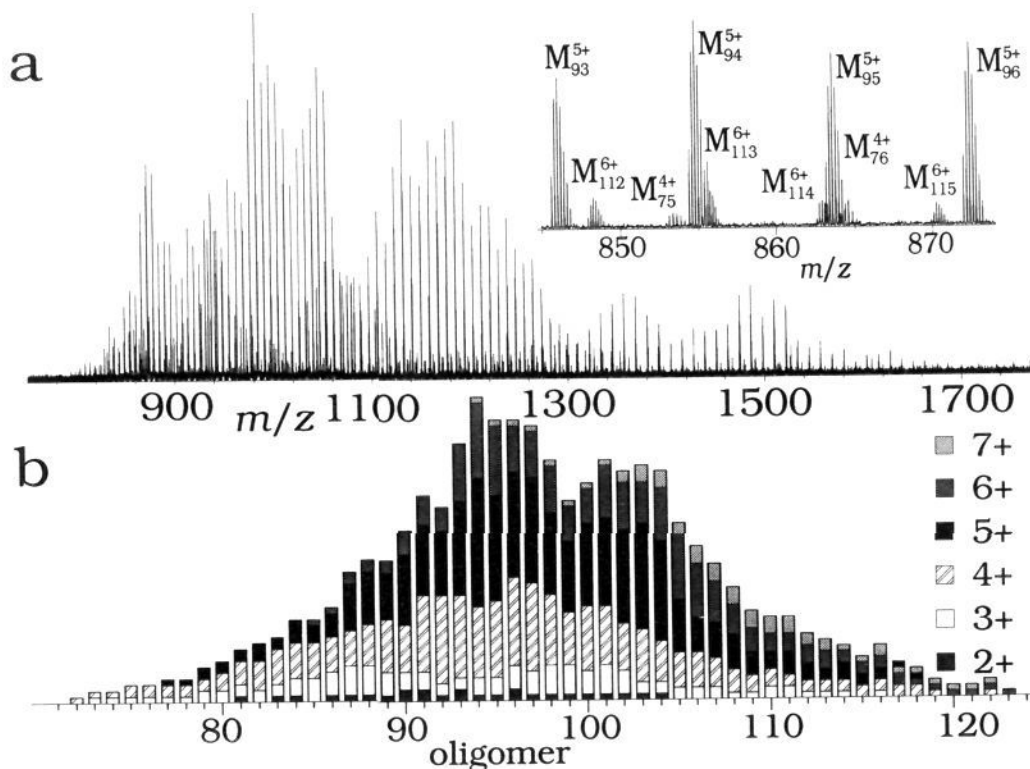


**Figure 1.** (a) ESI/FT mass spectrum of PEG 4500,  $RP = 10^5$ ; (b)  $M_r$  distribution from oligomer ion abundances summed over all isotopic peaks and charge states.

multiple peaks of different charges for each oligomer produce increasingly complex spectra with increasing mass. For example, the oligomeric ions 10 kDa<sup>10+</sup>, 11 kDa<sup>11+</sup>, and 12 kDa<sup>12+</sup> would all have nominal  $m/z$  values of 1000. For low-resolution instruments, these can only be distinguished if resolved peaks at  $m/(z \pm 1)$  or oligomeric peaks at  $(m \pm m_0)/z$  can be identified ( $m_0$  is the mass of a monomer unit).

For large biomolecules, this ESI problem has been alleviated using Fourier-transform mass spectrometry (FTMS)<sup>11</sup> that offers<sup>12</sup> routine RP of  $\sim 10^5$  even above 25 kDa.<sup>13</sup> This is sufficient at these masses to resolve <sup>12</sup>C/<sup>13</sup>C isotopic peaks, which provide a unit mass scale for direct determination of  $z$ , and hence  $m$ , from the  $m/z$  value of a multiply charged ion. FTMS also offers the multichannel advantage, allowing simultaneous measurement at high resolution of a wide range of  $m$  values (a 1-s data acquisition yields an ESI spectrum of 500 to  $> 10^5$  Da).<sup>12,13</sup> This study uses ESI/FTMS for direct measurement of isotopically resolved PEG oligomers, and thus of weight- and number-average molecular weight ( $M_w$  and  $M_n$ ) and polydispersity ( $M_w/M_n$ ).

## Experimental Section

PEG 4500 (Scientific Polymer Products, Inc., Ontario, NY) and PEG 14000 and PEG 20000 (Polysciences, Inc., Warrington, PA) were dissolved (20  $\mu$ M) in 50:50 H<sub>2</sub>O/MeOH containing mM NaOH. As

(11) Comisarow, M. B.; Marshall, A. G. *Chem. Phys. Lett.* **1974**, *25*, 282–283.

(12) Loo, J. A.; Quinn, J. P.; Ryu, S. I.; Henry, K. D.; Senko, M. W.; McLafferty, F. W. *Proc. Natl. Acad. Sci. U.S.A.* **1992**, *89*, 286–289. Beu, S. C.; Senko, M. W.; Quinn, J. P.; Wampler, F. M., III; McLafferty, F. W. *J. Am. Soc. Mass Spectrom.* **1993**, *4*, 557–565. Winger, B. E.; Hofstadler, S. A.; Bruce, J. E.; Udseth, H. R.; Smith, R. D. *J. Am. Soc. Mass Spectrom.* **1993**, *4*, 566–577.

(13) Speir, J. P.; Senko, M. W.; Little, D. P.; Loo, J. A.; McLafferty, F. W. *J. Mass Spectrom.* **1995**, *30*, 39–42. O'Connor, P. B.; Speir, J. P.; Senko, M. W.; Little, D. P.; McLafferty, F. W. *J. Mass Spectrom.* **1995**, *30*, 88–93.

described in detail elsewhere,<sup>13</sup> this solution was electrosprayed (needle, 3 kV) through a 110 C metal capillary (120 V) into a molecular beam skimmer (13 V), with the ions transmitted by quadrupoles (five stages of pumping) into a cylindrical open trapped ion cell controlled by an Extrel/Waters FTMS Odyssey data system. The ion beam was admitted to the cell during a N<sub>2</sub> pressure pulse peaking at  $3 \times 10^{-6}$  Torr, with the front trap plate at 4 V (back trap 1 V higher) for 2 s. Excitation at  $2 \times 10^{-9}$  Torr used a 50–150 kHz chirp of 110 V<sub>pp</sub> amplitude; detection used a 150 kHz bandwidth ( $m/z$  600–1800). The spectra shown represent the sums of 10 (PEG 4500), 20 (PEG 14000), and 30 (PEG 20000) measurements. Gel permeation chromatography utilized a Viscotek instrument with a styragel column at 25 °C, elution with THF, and a Viscotek refractometer/viscometer detector.

$M_w$  and  $M_n$  values were calculated by  $M_w = \sum m_i 2a_i / \sum m_i a_i$ , and  $M_n = \sum m_i a_i / \sum a_i$ , where  $m_i$  is the mass<sup>14</sup> of oligomer  $i$ , and  $a_i$  is its abundance, using a custom program on a Sun Sparc2 workstation. Illustrating the assignment of mass spectral peaks to individual oligomers, those at  $m/z$  853.4 (4+ isotopic spacing) and 870.3 (6+) (Figure 1, inset) represent the most abundant of the isotopic cluster peaks (<sup>13</sup>C<sub>2</sub> and <sup>13</sup>C<sub>3</sub>, respectively) and correspond to  $m_i = 3413.6$  and 5221.9; subtracting 2 or 3 <sup>13</sup>C (1.0034 Da) and 4 or 6 Na atoms (22.990 Da) yields  $m = 3319.6$  and 5080.9, so that for H(CH<sub>2</sub>CH<sub>2</sub>O)<sub>x</sub>OH (C<sub>2</sub>H<sub>4</sub>O = 44.0262, H<sub>2</sub>O = 18.011 Da),  $x = 74.99$  and 115.00, respectively.

## Results and Discussion

The ESI spectrum of PEG 4500 (Figure 1a) displays fully resolved isotopic peaks (inset). These show directly the number of charges ( $z$ ) from the number of isotopic peaks per  $m/z$  unit, identifying the 2+ to 7+ charge states, and thus provide mass ( $m$ ) values for every peak in this complex spectrum. These mass values correspond to  $(M + nNa)^{n+}$ , where  $M$  is H(CH<sub>2</sub>H<sub>4</sub>O)<sub>x</sub>OH, and show the almost exclusive adduction of Na<sup>+</sup>, not H<sup>+</sup>, due to the excess NaOH (the effect of NaOH

(14) Oligomer masses are reported as the mass of the most abundant isotopic peak, whose <sup>13</sup>C content is designated as <sup>13</sup>C<sub>*n*</sub>. This is within 0.01% of the average molecular weight using atomic weights from natural isotopic abundances.

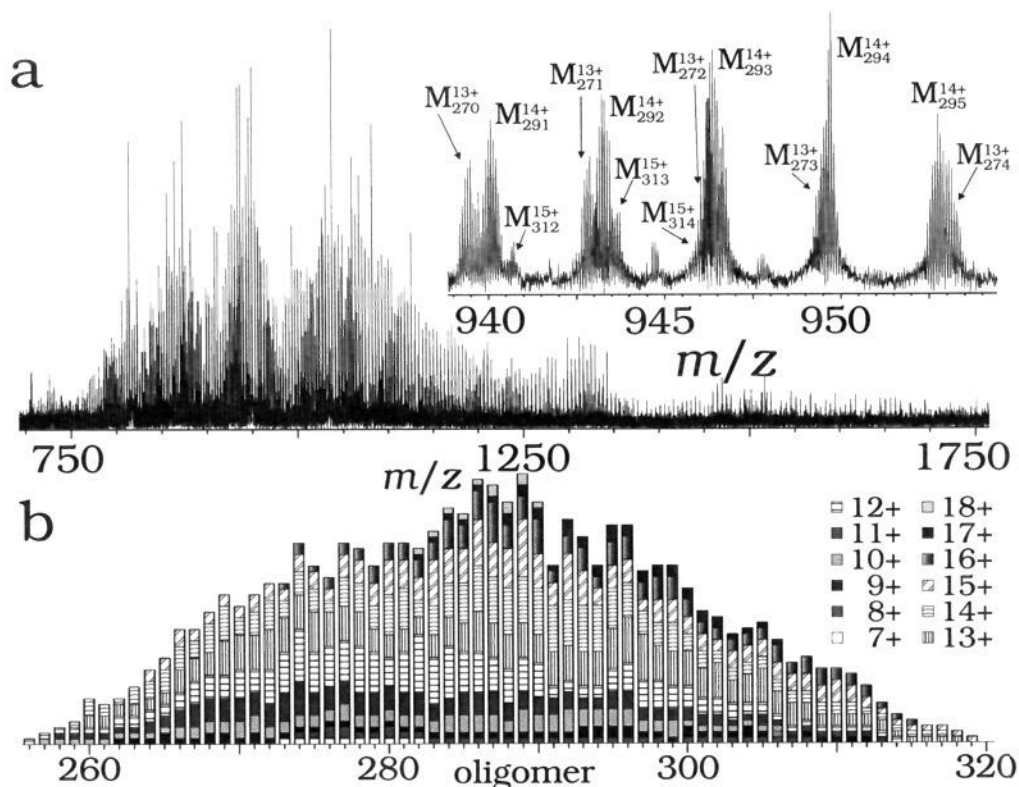


**Figure 2.** (a) ESI/FT mass spectrum of PEG 14000,  $RP = 10^5$ ; (b)  $M_r$  distribution from summed oligomer abundances.

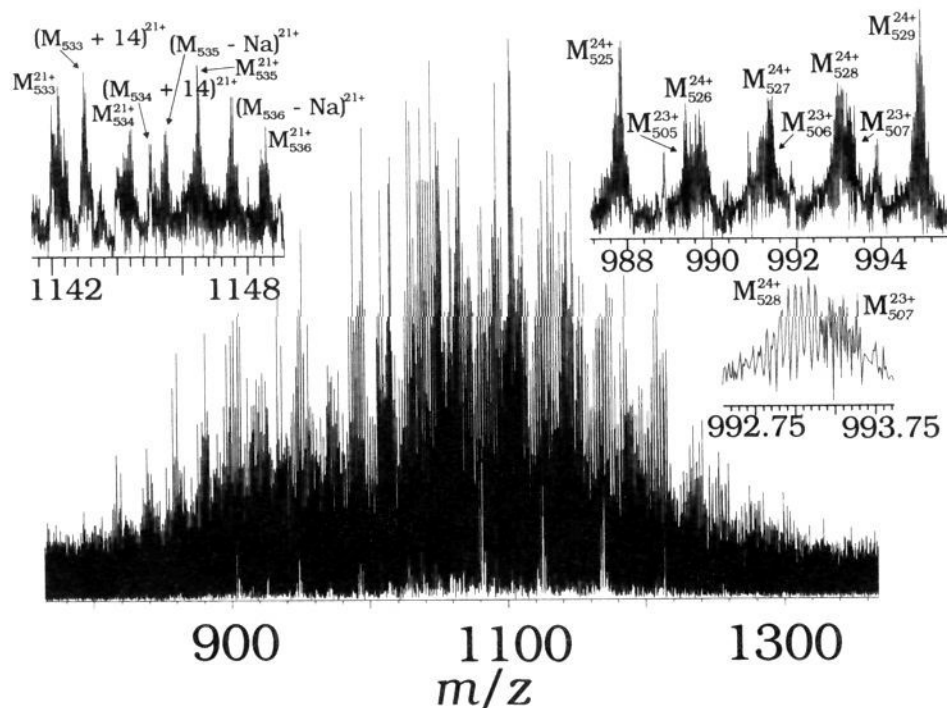


**Figure 3.** ESI/FT mass spectrum of PEG 20000,  $RP = 5 \times 10^4$ .

concentration was not studied). For  $M_{95}^{5+}$ , the  $(M + H + 4Na)^{5+}$  abundance at  $m/z$  859.3 is  $<5\%$  of that of  $(M + 5Na)^{5+}$  at  $m/z$  863.7 (most abundant isotopic peak,  $^{13}C_3$ ).<sup>14</sup> In a detailed manual interpretation of the spectrum, the total ion abundance due to each oligomer charge state was determined by summing the abundances of the corresponding isotopic peaks and charge state sums of the same  $x$  value totaled to provide the oligomer  $M_r$  distribution (Figure 1b). This clearly shows

oligomers ranging from 72 (3189.9 Da,  $^{13}C_2$ ) to 123 (5436.2 Da,  $^{13}C_3$ ), yielding  $M_w = 4349$ ,  $M_n = 4312$ , and  $M_w/M_n = 1.009$ .

The ESI spectrum of PEG 14000 (Figure 2) is more complex, with increasing overlap of the isotopic peaks of different charge states (Figure 2, inset). The oligomer values observed in the spectrum range from 256 to 319 (11295.7 Da,  $^{13}C_7$ , to 14070.4 Da,  $^{13}C_8$ ); the derived  $M_r$  distribution (Figure 2b) yielded  $M_w$

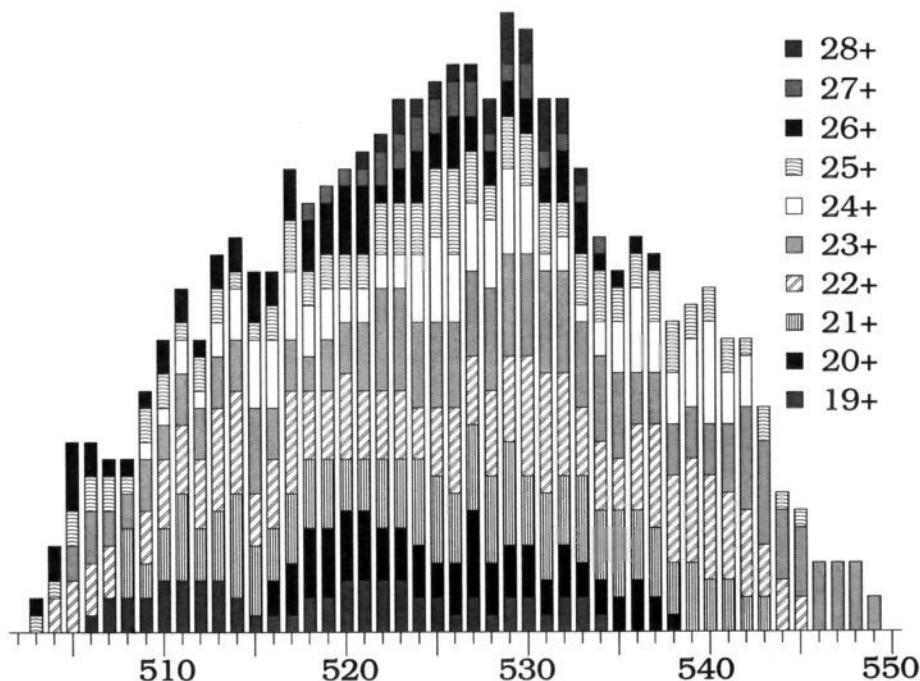


Figure 4.  $M_r$  distribution of PEG 20000 from Figure 3 abundances.

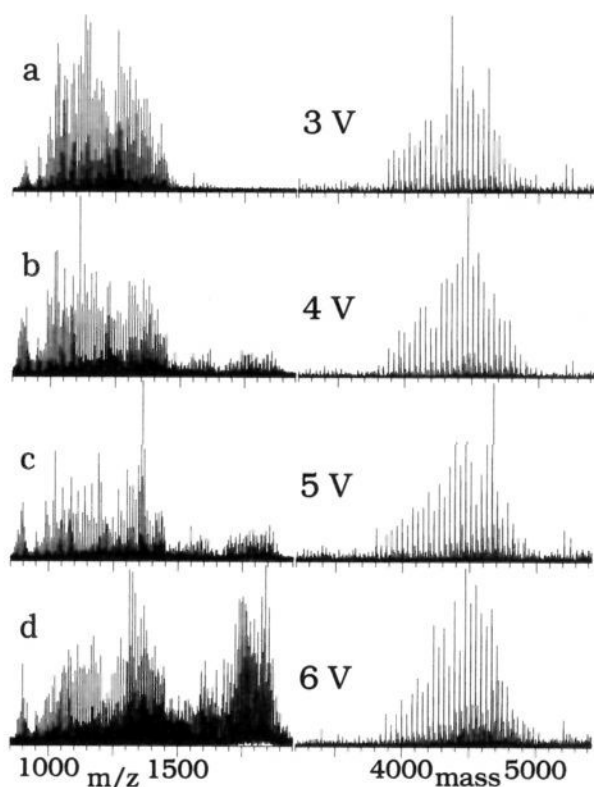


Figure 5. ESI/FT mass spectra of PEG 4500 versus trapping potential and (right column) after entropy deconvolution.

= 12661,  $M_n = 12663$ , and  $M_w/M_n = 1.002$ . PEG 20000 yields even higher complexity ( $\sim 5000$  peaks, Figure 3), but the resolving power of  $5 \times 10^4$  is still sufficient to identify 47 oligomers in 10 charge states (Figure 4) with oligomers from 503 to 549 (22176 Da,  $^{13}\text{C}_{13}$ , to 24202 Da,  $^{13}\text{C}_{14}$ ). Although the signal/noise ratio of individual peaks is correspondingly attenuated, the relevant  $M_r$  information can still be determined;  $M_w = 23174$ ,  $M_n = 23165$ , and  $M_w/M_n = 1.0004$ . Note that Na adduction is not complete (left inset), with a  $\text{Na}^+$  charge

carrier in some oligomeric ions replaced with a proton (and, also, possibly  $\text{K}^+$ ; see below).

**Impurities.** Isotopic resolution makes possible identification of heterogeneous polymers or other impurities. For example, contamination of the ethylene oxide monomer with propylene oxide should yield heteropolymeric oligomers. Consider the  $M_{294}^{14+}$  isotopic peaks centered at  $m/z$  949.6 in Figure 2 (inset); an oligomer for which one of these 294  $-\text{CH}_2\text{CH}_2\text{O}-$  groups (44 Da) is replaced with a  $-\text{CH}_2\text{CH}(\text{CH}_3)\text{O}-$  group (58 Da) should produce peaks centered at  $m/z$  950.6 (extra  $m/z = 14/14^+$ ). The abundances of these peaks, which are difficult to distinguish from noise, are  $\leq 5\%$  of those of  $M_{294}^{14+}$ . This demonstrates that the PEG 14000 sample contains at most 0.02% ( $1/294 \times 5\%$ ) monomer units containing an extra  $\text{CH}_2$ . In the PEG 20000 sample, the  $M_{533}^{21+}$ – $M_{534}^{21+}$  isotopic peaks at  $m/z$  1142–1144 (Figure 3; left inset) do have significant peaks  $\sim 14$  Da higher. The relative abundance of these +14 Da peaks throughout the PEG 20000 spectrum is quite variable (consistent with poor ion statistics), averaging 14% or 0.03% ( $14\% \times 1/525$ ) of the  $-\text{CH}_2\text{CH}(\text{CH}_3)\text{O}-$  monomer unit. However, part of this could be due to one  $\text{K}^+$  ion replacing a  $\text{Na}^+$  ion that would produce a second isotopic distribution 16 mass units higher, a difficult distinction at this isotopic peak multiplicity and signal/noise level.

**Mass Discrimination.** Detecting ions of different masses with equal probabilities is difficult for most MS instrumentation. The complex ESI/FTMS process is no exception;<sup>15</sup> for PEG 4500, changing the trapping potentials that capture ions in the FTMS cell yields dramatic changes in abundance vs  $m/z$  value (Figure 5, left column). The trapping procedure samples a narrow range of ion kinetic energies that depend on collisions in the ESI process and in ion injection; a wider range of kinetic energies could be trapped by modulating either the kinetic energy of the ions<sup>10e</sup> or the trapping potential. Although higher trapping potentials substantially favor the abundance of lower  $z$  ions, the  $m$  value distributions are still quite similar (Figure

(15) Campbell, V. L.; Guan, Z.; Laude, D. A. *J. Am. Soc. Mass Spectrom.* **1994**, *5*, 221–229. Hogan, J. D.; Laude, D. A. *J. Anal. Chem.* **1992**, *64*, 763–769. Hofstadler, S. A.; Beu, S. C.; Laude, D. A., Jr. *Anal. Chem.* **1993**, *65*, 312–316.

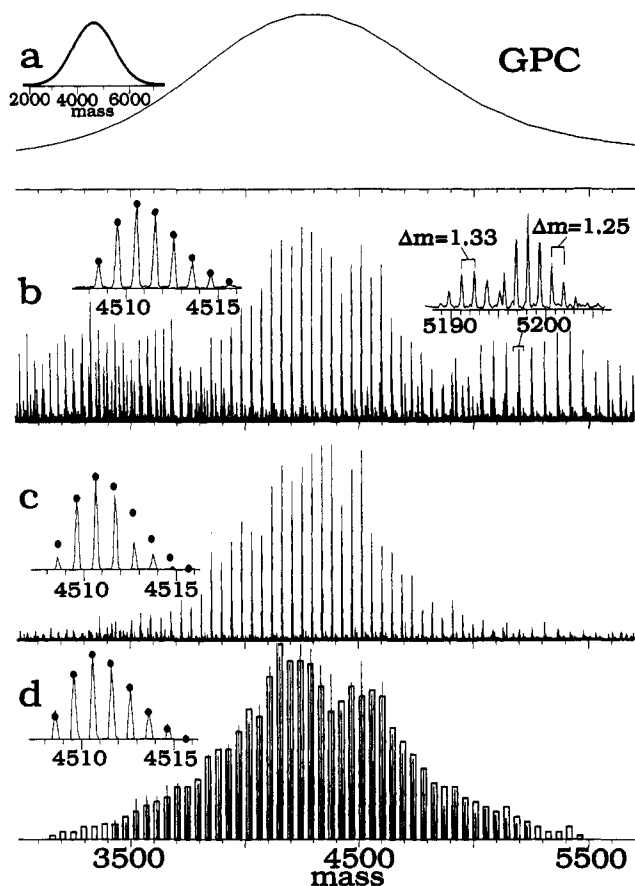


**Figure 6.**  $M_r$  distribution of PEG 4500: (a) from gel permeation chromatography and from deconvolutions, (b) geometric, (c) entropy, and (d) geometric with entropy filtering (rectangles, data of Figure 1b). Insets: isotopic peaks, circles are abundances predicted by theory.

5, right column), with  $M_n$  values of 4339, 4395, 4371, and 4400 for 3, 4, 5, and 6 V trapping. This average of 4376, standard deviation  $\pm 28$  (0.6%), is comparable to the Figure 1b value of  $M_n = 4312$  for the same sample measured two months earlier.

The charge state data also exhibit mass discrimination (Figure 1b, 4 V trapping). With increasing charge values, the higher mass ions show an increasing relative abundance; the 3+, 4+, 5+, and 6+ charge states yield increasing  $M_w$  ( $M_n$ ) values of 4200 (4137), 4271 (4235), 4378 (4330), and 4482 (4457), and  $M_w/M_n$  of 1.015, 1.009, 1.011, and 1.006.<sup>16</sup> The relative standard deviation of the 3+ to 6+  $M_n$  values from Figure 1b is 3.2%. In a similar approach, averaging MALDI spectra recorded at different FTMS trapping times also reduces mass discrimination;<sup>8e</sup> from 80 to 130 ms,  $M_n$  rose from 2947 to 3545, relative standard deviation 7.3%. The much higher variation in initial ion kinetic energies from MALDI vs ESI should result in higher MALDI mass discrimination in time-of-flight as well as FTMS instruments; a poly(methyl methacrylate) sample yielding  $M_n = \sim 3200$  by GPC gave  $M_n = \sim 2000$  by MALDI/MS.<sup>8f</sup>

**Deconvolution.** Although the summed spectra of Figures 1a, 2a, and 3 were each measured in minutes, the identification from these spectra of all charge states of all oligomers (Figures 1b, 2b, and 4) was very laborious. Two deconvolution algorithms<sup>17</sup> are widely used for automation of such data interpretation. Although these programs calculated the MW distributions quickly, they yielded remarkably different results

(16) Another possible discrimination gives somewhat bimodal distributions with lowered abundances at  $m = \sim 4100$  for 3+,  $\sim 4200$  for 4+, and  $\sim 4400$  for 5+ and 6+; this is not apparent from gel permeation chromatography (GPC, Figure 6a), and is difficult to discern in the 14 and 20 kDa data, Figures 2b and 4.

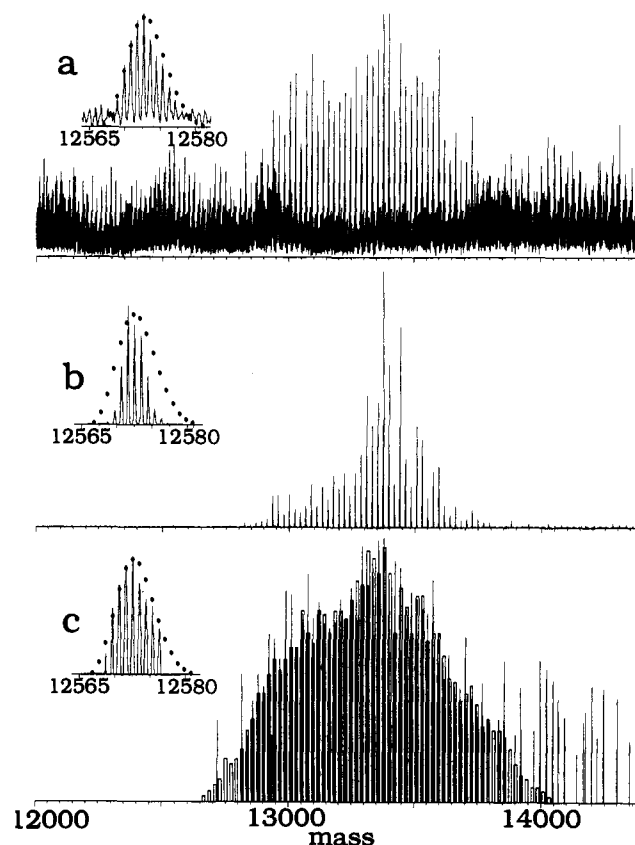


**Figure 7.**  $M_r$  distribution of PEG 14000 from deconvolutions: (a) geometric, (b) entropy, and (c) geometric with entropy filtering (rectangles, data of Figure 2b).

for both PEG 4500 (Figures 6a,b) and PEG 14000 (Figures 7a,b), and both gave meaningless results (not shown) for the complex PEG 20000 spectrum.

For PEG 4500 with Mann's geometric deconvolution<sup>17a</sup> (Figure 6b), the 4–5 kDa peaks show the expected 44 Da oligomer spacing ( $-\text{CH}_2\text{CH}_2\text{O}-$ ). However, prominent spacings at low (and high) mass are 67% and 80% (125% and 133%) of this, as are those of the corresponding isotopic peaks (Figure 6a, right inset) that should have unit Da spacing (left inset). For example, the false 5190–5196 Da isotopic peaks (1.33 Da spacing) arise in large part from  $M_{88}^{3+}$  ( $^{13}\text{C}_2$ ) at  $m/z$  1321.1, for which the algorithm has incorrectly assigned  $z = 4$  and  $m = 5192.4$  ( $^{13}\text{C}_2$ ), plus isotopic peaks at  $\pm 1.33$ ,  $\pm 2.67$  Da, etc. Similarly, for 5198  $\pm 1.25$ ,  $\pm 2.50$  Da peaks, the algorithm has matched the 4+ peak at  $m/z$  1062.6  $\pm 1$ ,  $\pm 2$  ( $M_{94}^{4+}$ ,  $^{13}\text{C}_2$ ) as if it were 5+. Note that abundances for both peak groups are similar to those of the 4508–4515 Da isotopic peaks; small additional contributions arise by the algorithm assigning incorrectly high  $z$  values to a few of the multitude of oligomeric and isotopic peaks. This mechanism obviously produces far more artifact peaks for PEG 14000 (Figure 7a), whose peaks are much more numerous and highly charged.

Such artifact peaks are greatly reduced by Reinhold's entropy penalty method<sup>17b</sup> (Figures 6c and 7b), but the distributions yielded by this approach show significant, and severe (PEG 14000), abundance distortion both for the oligomers (vs rectangles, Figures 6d and 7c) and for their individual isotopic distributions (left inset). In minimization of the false peaks of the geometric deconvolution,<sup>17a</sup> the entropy method distorts the

(17) (a) Mann, M.; Meng, C. K.; Fenn, J. B. *Anal. Chem.* **1989**, *61*, 1702–1708. (b) Reinhold, B. B.; Reinhold, V. N. *J. Am. Soc. Mass Spectrom.* **1992**, *3*, 207–215.

sum of the abundances of the charge states. Also, neither method finds all oligomers of the raw data (e.g.,  $M_{75}^{4+}$ , Figure 1 inset).

**Improved Deconvolution.** Minimization of these distortions was sought by merging the deconvolution approaches, combining oligomeric masses from the entropy deconvolution data with the intensities from the geometric deconvolution data; to further reduce the number of false peaks, an isotopic spacing criterion was added requiring an included data point to have a neighbor separated by 1.0 Da in mass (threshold at 1.1 signal/noise). The resulting distribution (Figure 6d) for PEG 4500 agrees well (average difference <10%) with the Figure 1b data (rectangles) from human interpretation; however, the calculated distribution for the PEG 14000 spectrum (Figure 7c), although improved, contains numerous artifact peaks. None of these deconvolution approaches was successful on the PEG 20000 spectrum. Further restrictions to the deconvolutional algorithms for polymers should include those used in human reduction of the data, such as correlation for monomer unit mass.

**Average Molecular Weight Values.** The PEG 4500 sample was also subjected to gel permeation chromatography (GPC)<sup>1</sup> (Figure 6a), whose  $M_r$  scale calibration (typically poorest below 10 kDa) could be in error by  $\pm\sim 300$ . The agreement in distribution between Figures 6a and 6d, although qualitative, is reassuring;  $M_w$  ( $M_n$ ) values are 4140 vs 4349 (4037 vs 4312), respectively, with  $M_w/M_n = 1.026$  vs 1.009. However,  $M_r$  values for the GPC data range from  $\sim 2000$  to  $\sim 7000$ , vs 3100 to 5500 for ESI/FTMS (Figure 6d). This difference could be due to GPC noise levels or peak broadening<sup>1</sup> and/or other FTMS ion repulsion,<sup>15</sup> although the data above indicate the latter is of

lower importance.  $M_r$  distributions from the mass spectra of a few GPC fractions of the PEG 4500 would delineate the discriminations of GPC vs ESI/FTMS even more clearly.

## Conclusions

Although present ESI solubility restrictions will have to be resolved for extensive application to polymeric materials, ESI/FTMS of PEG polymers as large as 23 kDa allows direct measurement of individual oligomers, including those from copolymerization and side reactions. The  $m/z$  discrimination appears to be less than in MS measurements with MALDI or other instruments, and averaging the distributions from multiple charge states further minimizes errors in mass abundances. Errors should be reduced further by calibration with mixtures of monodisperse samples. Interpretation of the complex ESI/FTMS spectra is simplified with a combination of deconvolution algorithms modified to minimize artifact peaks while retaining accurate abundance information.

**Acknowledgment.** The authors are grateful to J. Frechet, D. Y. Sogah, and F. H. Winslow for advice, to R. Puts for assistance in obtaining the GPC results, to B. B. Reinhold for assistance in implementation of his deconvolution technique, to S. C. Beu, R. A. Chorush, R. M. A. Heeren, Neil L. Kelleher, D. P. Little, M. W. Senko, J. P. Speir, B. E. Winger, and T. D. Wood for helpful discussions and/or experimental assistance, and to the National Institutes of Health (Grant No. GM16609) for generous financial support.

JA952126F